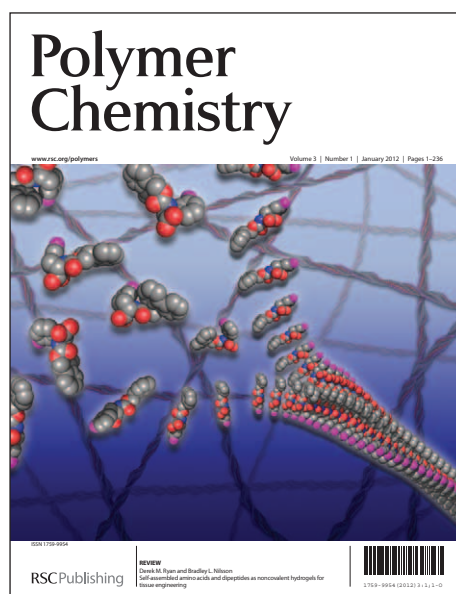


Polymer Chemistry

Accepted Manuscript

This article can be cited before page numbers have been issued, to do this please use: G. Liou, C. Chen and Y. Hu, *Polym. Chem.*, 2013, DOI: 10.1039/C3PY00500C.



This is an *Accepted Manuscript*, which has been through the RSC Publishing peer review process and has been accepted for publication.

Accepted Manuscripts are published online shortly after acceptance, which is prior to technical editing, formatting and proof reading. This free service from RSC Publishing allows authors to make their results available to the community, in citable form, before publication of the edited article. This *Accepted Manuscript* will be replaced by the edited and formatted *Advance Article* as soon as this is available.

To cite this manuscript please use its permanent Digital Object Identifier (DOI®), which is identical for all formats of publication.

More information about *Accepted Manuscripts* can be found in the [Information for Authors](#).

Please note that technical editing may introduce minor changes to the text and/or graphics contained in the manuscript submitted by the author(s) which may alter content, and that the standard [Terms & Conditions](#) and the [ethical guidelines](#) that apply to the journal are still applicable. In no event shall the RSC be held responsible for any errors or omissions in these *Accepted Manuscript* manuscripts or any consequences arising from the use of any information contained in them.

Linkage and Acceptor Effect on Diverse Memory Behavior of Triphenylamine-Based Aromatic Polymers

Chih-Jung Chen, Yi-Cheng Hu, and Guey-Sheng Liou*

*Functional Polymeric Materials Laboratory, Institute of Polymer Science and Engineering,
National Taiwan University, 1 Roosevelt Road, 4th Sec., Taipei 10617, Taiwan*

* Corresponding author. E-mail: gслиou@ntu.edu.tw

ABSTRACT: New functional triphenylamine-based (TPA-based) aromatic polyether (**OXPE**) derived from 2,5-bis(4-fluorophenyl)-1,3,4-oxadiazole and 4,4'-dihydroxytriphenylamine and polyester (**6FPET**) derived from 4,4'-(hexafluoroisopropylidene)bis(benzoyl chloride) and 4,4'-dihydroxytriphenylamine were synthesized and used for memory device application. To get more insight into the relationship between linkage group and memory behavior, polyamide **6FPA**, polyimide **6FPI**, and the corresponding isomer **6FPI'** were also synthesized and investigated their memory properties. The linkage effects of polyether, polyester, polyamide, and polyimide are expected to reveal different retention time of the resulted polymer memory devices due to their different structural conformation, dipole moment, HOMO, and LUMO energy levels. **OXPE**, **6FPA**, and **6FPET** with non-planar linkage structure but different LUMO energy levels possess SRAM behavior with different retention time, 2 min, 5 min, and 6 min, respectively. **6FPI** with planar linkage group exhibits DRAM property while the corresponding isomer **6FPI'** reveals insulator behavior due to the sustaining of charge transfer complex is difficult. Furthermore, to illustrate the linkage and acceptor effect systematically, TPA-based sulfonyl-containing polymers with the same linkages were also added into discussion.

Introduction

Due to the exponential growth of information communication and the miniaturization of electronic devices, polymeric memory materials have attracted increasing attention over the years since the first one published by Sliva et al. in 1970.¹ Comparing with conventional inorganic memory materials, polymeric materials have numerous advantages such as ease of miniaturization, tailored properties through molecular design, low-cost, solution processability, flexibility, and three-dimensional stacking capability for practical use.² As a promising alternative to inorganic semiconductor-based memory, polymeric memory materials store information in the form of high (ON) and low (OFF) current state in place of the amount of charges stored in a cell of silicon devices. In the starting stage of polymer memory applications, polymers were used as polyelectrolytes or matrices in a doped system.³ To advance the function of polymers for memory devices further, the design and synthesis of the polymers with specific structures that can provide expected memory properties within single polymer chain is an important and crucial issue.

For resistive type memory materials, electron donor-acceptor polymers are considered as suitable materials because charge transfer (CT) between the donor and acceptor moieties can give rise to a high conductive state.⁴ Donor-acceptor type polymers including conjugated polymers,⁵ non-conjugated pendent polymers,⁶ polymer composites,⁷ and functional polyimides⁸ have been reported widely with all kinds of chemical structures. Among all the studied donor-acceptor systems, aromatic polyimides are promising candidates for memory device applications due to the excellent thermal dimensional stability, chemical resistant, mechanical strength, and high ON/OFF current ratio resulted from the low conductivity in the OFF state. Although aromatic polyimides have superior properties, they are generally restricted by limited solubility in most organic solvents and their high glass transition (T_g) or melting temperatures caused by the high crystallinity and high stiffness of the polymer backbones, and charge transfer complex formation. To overcome the solubility problem of polyimides, non-coplanar triphenylamine (TPA) group was introduced into polyimides and enhanced the solution processability. Furthermore, TPA could act as a donor and facilitate the CT behavior of polyimide, therefore, a series of TPA-based polyimides with different substituted groups and dianhydrides were prepared for memory devices.^{4a,9}

In addition to polyimides, TPA-based aromatic polyamides and polyesters were also characterized as highly thermally stable polymers with a favorable balance of physical and chemical properties.¹⁰ In our previous study, TPA-based polyamide and polyester revealed

different volatile memory characteristics from polyimide due to the difference of linkage, dipole moment, HOMO, and LUMO energy levels among these polymers.¹¹ In addition to the conformational changes of flexible linkage between the donor and acceptor moieties of aromatic polyamide and polyester, the increment of torsional displacement induced by charge transfer would produce a potential energy barrier for the back charge transfer that resulted in the longer retention time.¹² It is interesting to get more insight into the relationship between memory behaviors and linkage groups of these functional polymers.

Furthermore, TPA-containing aromatic polyethers could also be obtained as high performance polymers with excellent processability, electroactive and electrochromic properties.¹³ However, in our previous study, TPA-based sulfonyl-containing polyether **DSPE** exhibited only insulator behavior due to the large band gap and weak CT capability.^{11b} According to previous literatures, memory device with thinner thickness is advantageous to reduce switch-on voltage and reveal memory behavior.^{9b,9c,11a} In this study, we therefore synthesized oxadiazole-containing polyether **OXPE** derived from 2,5-bis(4-fluorophenyl)-1,3,4-oxadiazole and 4,4'-dihydroxytriphenylamine with stronger acceptor moiety than **DSPE**, and also reduced film thickness of the resulting polyethers to achieve the memory characteristics for the first time. TPA-containing polyimides could be synthesized either from TPA-based diamine or TPA-based dianhydride to have different direction of polyimide linkages. We also predicted that the direction of polyimide linkages should affect the CT behavior and the resulting memory property. Therefore, the corresponding isomer **6FPI'** of **6FPI** was synthesized in this present work to demonstrate isomeric effect on the memory property. In order to illustrate the linkage and acceptor effect systematically, polyamide **6FPA** and new functional polyester **6FPET** derived from 4,4'-(hexafluoroisopropylidene)bis(benzoyl chloride) and 4,4'-dihydroxytriphenylamine were prepared for detailed discussion and compared with the corresponding sulfonyl-containing polymers.

Results and Discussion

Polymer Synthesis and Characterization. The TPA-based new polyether **OXPE** was prepared by the reaction of diol monomer **1** with **OXDF** in NMP at 150 °C with toluene to remove water during the formation of phenoxide anions, followed by 170 °C, 180 °C, and 190 °C reaction temperature segments as shown in Figure 1. The formation of polyether **OXPE** was confirmed by IR spectroscopy showing characteristic absorption bands at around 1500-1600 (C=N), and 1232 cm⁻¹ (C-O-C) (Figure S1a). Anal. Calcd. (%) for **OXPE** were C, 77.56;

H, 4.27; N, 8.48 and found C, 75.11; H, 3.82; N, 8.27. The TPA-based new polyester **6FPET** was synthesized by the reaction of diol monomer **1**^{14a} with **6FAC** in *o*-dichlorobenzene at 180 °C as shown in Figure 1. The formation of polyester **6FPET** was also confirmed by IR spectroscopy showing characteristic ester carbonyl absorption band at around 1737 cm⁻¹ (C=O) (Figure S1b). Anal. Calcd. (%) for **6FPET** were C, 66.35; H, 3.34; N, 2.21 and found C, 64.56; H, 2.93; N, 2.15. Synthesis and characterization of the **6FPA**, **6FPI**, and **6FPI'** has been described previously.^{14c,15} The inherent viscosity and GPC analysis data of the TPA-based aromatic polymers were summarized in Table S1. The obtained polymers have inherent viscosities in the range of 0.27-0.75 dL/g with weight-average molecular weights (M_w) and polydispersity (PDI) of 62,000-166,000 Da and 1.78-2.58, respectively, relative to polystyrene standard. The solubility behavior of **OXPE** and **6FPET** was investigated qualitatively and the results were listed in Table S2. **OXPE** and **6FPET** exhibited excellent solubility not only in polar aprotic organic solvents such as NMP and DMAc, but also in less polar solvent such as CHCl₃ and THF. The excellent solubility can be attributed to the existence of the bulky TPA unit which limits the intermolecular interactions. The excellent solubility is conducive to fabricate memory device by solution process.

Thermal Properties. The thermal properties of new functional polymers **OXPE** and **6FPET** were investigated by TGA and DSC, and the results were summarized in Table 1. Typical TGA and DSC curves of **OXPE** and **6FPET** are depicted in Figure S2. Both of **OXPE** and **6FPET** exhibited good thermal stability with insignificant weight loss up to 350 °C under nitrogen or air atmosphere. The 10 % weight-loss temperatures of **OXPE** and **6FPET** were recorded of 500 °C, 480 °C in nitrogen, and 500 °C, 465 °C in air, respectively. The amount of carbonized residue (char yield) of **OXPE** and **6FPET** in nitrogen atmosphere were 49 % and 50 % at 800 °C, which could be ascribed to their high aromatic content. Limiting Oxygen Index (LOI) of **OXPE** and **6FPET** calculated by char yield were 37 and 38, respectively. The glass transition temperatures (T_g) of **OXPE** and **6FPET** were 206 °C and 193 °C, respectively. The excellent thermal properties were advantageous to memory device which may release heat during operation.

Optical and Electrochemical Properties. UV-vis absorption spectra of **OXPE**, **6FPET**, **6FPA**, **6FPI**, and **6FPI'** are shown in Figure 2 and the onset wavelengths of optical absorption were utilized to obtain the optical energy band gap (E_g) of these polymers. The electrochemical behavior of these polymers was investigated by cyclic voltammetry conducted by film cast on an ITO-coated glass substrate as the working electrode in dry

acetonitrile (CH_3CN) containing 0.1 M of TBAP as an electrolyte under nitrogen atmosphere. The typical cyclic voltammograms for these polymers are depicted in Figure 3. There is one oxidation redox couple for all polymers, and the onset oxidation of these five polymers exhibited at 0.69, 1.00, 0.71, 1.01, and 1.27 V, respectively. The optical and electrochemical properties of these five polymers are summarized in Table 2 along with TPA-based sulfonyl-containing polymers, and the optical energy band gaps (E_g) estimated from the onset optical absorption are 3.27, 3.06, 2.91, 2.58, and 2.53 eV, respectively. **6FPI** and **6FPI'** have similar low energy gaps due to the strong charge-transfer effect between TPA moiety and phthalic imide ring. The LUMO energy levels of these five polymers decrease in the order of **OXPE**, **6FPA**, **6FPET**, **6FPI**, and **6FPI'**. Reduction cyclic voltammograms were utilized to calculate the electrochemical LUMO energy levels of **6FPI** and **6FPI'** as shown in Figure S3, and the results were also summarized in Table 2. The HOMO energy levels of **OXPE**, **6FPET**, **6FPA**, **6FPI**, and **6FPI'** estimated from the onset of their oxidation in CV experiments were 5.13, 5.44, 5.15, 5.45, and 5.63 eV, respectively (on the basis of ferrocene/ferrocenium 4.8 eV below the vacuum level with $E_{\text{onset}} = 0.36$ V). Comparing the acceptor effect systematically, the corresponding sulfonyl-containing polymers generally have lower LUMO energy levels than hexafluoroisopropylidene-containing (6F) series polymers with the same linkage. Besides, **OXPE** has lower LUMO energy levels than **DSPE** due to the stronger acceptor oxadiazole moiety.

Memory Device Characteristics. The memory behaviors of these TPA-based aromatic polymers were depicted by the current-voltage (I-V) characteristics of an ITO/polymer/Al sandwich device as shown in Figure 4. Within the sandwich device, polymer film was used as an active layer between Al and ITO as the top and bottom electrodes. To exclude the effect of the polymer film thickness on memory properties, a standard thickness (50 nm) was used without specific mention. Figure 4a reveals I-V characteristics of **6FPET**. The device based on **6FPET** could not be switched to the ON state and stayed in the OFF state with a current range 10^{-13} – 10^{-14} A in the positive sweep up to 6 V (not shown). However, a sharp increase in the current could be observed at -3.6 V during the negative sweep, indicating that the device undergoes an electrical transition from the OFF state to the ON state (writing process). The device also remained in the ON state during the subsequent negative (the second sweep) and positive scans (the third sweep). Thus, this **6FPET** memory device could not be reset to the initial OFF state by the introduction of a reverse scan and is thus non-erasable. The fourth sweep was conducted after turning off the power for about 6 minutes and it was found that

the ON state had relaxed to the steady OFF state without an erasing process. During the fourth sweep, the device could be switched to the ON state again at the threshold voltage of -3.3 V. Thus, the device could open to the ON state again and was rewritable. The 6 minutes retention time at the ON state yet volatile as well as the randomly accessible ON and OFF states in each ITO/**6FPET**/Al device are similar to the data remanence behavior of SRAM.^{12a} Figure 4b reveals I–V characteristics of **6FPA** which have similar SRAM memory properties with different retention time of 5 minutes.

The memory device of **6FPI** switched from 10^{-13} - 10^{-14} to 10^{-5} A at the threshold voltage of -3.5 V in the negative sweep and the ON state could be read by the subsequent negative (the second sweep) and positive scans (the third sweep) as shown in Figure 4c. The ON state would return to OFF state in 1 min after removing the applied voltage then subsequently switch to ON state again at the threshold voltage of -3.4 V, implying the similar volatile **DRAM** behavior as published before.^{4a} However, the corresponding **6FPI'** kept at low-conductivity (OFF) state during the positive and negative scan as shown in Figure 4d. Thus, **6FPI'** showed no memory but insulator behavior. Figure 5 and Figure 6 depict the I-V results of **OXPE** and **DSPE** with different thickness, respectively. **OXPE** exhibited insulator, SRAM, and SRAM properties with the corresponding thickness around 50, 40, and 30 nm, respectively. Meanwhile, **DSPE** only exhibited DRAM behavior with film thickness around 30 nm. Thus, these TPA-based aromatic polymers exhibited not only diverse memory properties but also high ON/OFF current ratios of 10^8 - 10^9 . The high ON/OFF current ratio is advantageous to reduce misreading probability between ON state and OFF state.

Theoretical Analysis and Switching Mechanism. In order to get more insight into the different memory behavior of the present TPA-based aromatic polymer devices, molecular simulation on the basic unit was carried out by DFT/B3LYP/6-31G(d) with the Gaussian 09 program. The charge density isosurfaces of the basic unit and the most energetically favorable geometry of **OXPE**, **6FPET**, **6FPA**, **6FPI**, and **6FPI'** were summarized in Figure 7, and the simulation results of TPA-based sulfonyl-containing polymers were listed in Figure S4. The LUMO energy levels calculated by molecular simulation were in agreement with the experimental values tendency and could be utilized as an evidence to indicate the electron-withdrawing intensity of various acceptors and donor-acceptor interaction capability via different linkage group. For these TPA-based polymer systems, the HOMO energy levels were located mainly at the electron-donating TPA moieties, while the LUMO energy levels were generally located at the corresponding electron-withdrawing units. In the case of **6FPI**

and **DSPI**, the distribution LUMO energy levels were within the dianhydride and imide ring moiety due to their strong electron-withdrawing capability. Comparing to **6FPI** and **DSPI**, the distribution LUMO energy level of **6FPI'** was also located at the imide ring moiety. However, due to the direction of polyimide linkages between **6FPI'** and other polyimides is different, the HOMO and LUMO energy levels of **6FPI'** almost overlap and result in the poor sustaining ability for CT complex. The LUMO energy levels of the polyesters and polyamides were found at the ester and amide linkage groups. However, the poorest charge separation phenomena of polyether **OXPE** and **DSPE** could be predicted and observed in the analysis of molecular simulation, indicating the weakest electron-withdrawing capability resulted from the isolated ether linkage group. Comparing to other polymers, LUMO2 of **OXPE** and **DSPE** were distributed with overlapping around the whole basic unit that could also be indicated as the evidence for the poor sustaining ability for CT complex.

According to previous literatures,^{4a} when the applied electric fields reach the switching-on voltage, some electrons at the HOMO accumulate energy and transit to the LUMO5 (LUMO4 for **6FPET**) with the highest probability because of overlapping of the HOMO and LUMO5 resulting in an excited state. In addition, electrons at the HOMO can also be excited to other intermediate LUMOs with lower energy barrier belonging to the acceptor units. Thus, CT occurs through several courses to form the conductive CT complexes, including indirectly from the LUMO5 through intermediate LUMOs and then to the LUMO, or from the intermediate LUMOs to the LUMO, and directly from the HOMO to the LUMO. Based on this proposed mechanism, when the negative sweep was conducted, the hole injected from the bottom electrode ITO to the HOMO of the polymer due to the lower band gap between ITO (-4.8 eV) and HOMO.¹⁶ In contrast, during the positive sweep, the hole is difficult to be injected from the top electrode Al into the HOMO of these polymers because of the larger energy gap between the work function of Al (-4.2 eV) and HOMO of the polymers, thus the memory device could not be switched to the ON state.

Furthermore, the stability of the CT complex is important and is relative to the retention time of the memory device. Therefore, **OXPE** and **DSPE** showed only insulator behavior with 50 nm thickness due to the large band gap and weak CT capability. Comparing to **DSPE**, **OXPE** with stronger acceptor oxadiazole moiety revealed longer retention time (SRAM) than **DSPE** (DRAM) in the case of decreasing thickness to 30 nm. In addition, **6FPA** exhibited longer retention time than **6FPI** contributing to the conformation effect and higher dipole moment. The conformation of the phenyl ring with amide linkage is not a planar structure

which may block the back CT occurring, and higher dipole moment of **6FPA** also facilitates to stabilize the CT complex. **6FPET** having a similar non-planar structure to **6FPA** but lower LUMO than **6FPA** leads to even longer retention time than **6FPA**. As described before, the HOMO and LUMO charge density isosurfaces of **6FPI'** almost overlap and result in the poor sustaining ability for CT complex. Therefore, although chemical structure of **6FPI'** was similar to **6FPI**, **6FPI'** only has insulator behavior. The memory properties of TPA-based aromatic polymers are summarized in Figure 8. Generally, polymers with flexible linkages, lower LUMO energy levels, and higher dipole moments will facilitate the stability of CT complex, and the retention time of polymer memory devices is very dependent on the stability of CT complex. Therefore, the sulfonyl-containing polymers generally show longer retention time than 6F series polymers with the same linkages due to the stronger acceptor effect. For example, **DSPI** possess SRAM property while **6FPI** have DRAM property. **DSPET** and **DSPA** have longer retention time than **6FPET** and **6FPA**, respectively.

Conclusion

In summary, new functional TPA-based aromatic polyether **OXPE** and polyester **6FPET** were successfully synthesized for the first time as memory device application. For comparison, **6FPA**, **6FPI**, and **6FPI'** were also prepared for systematically investigating the relationship between chemical structure and memory behavior. To get more insight into acceptor effect on memory behavior, sulfonyl-containing polymers were also added into discussion. **OXPE** exhibited the 2 minutes retention time SRAM property with thickness 30 and 40 nm, while **DSPE** could only has DRAM behavior when the film thickness was reduced to 30 nm. **6FPET** and **6FPA** showed SRAM properties with different retention times of 6 min, and 5 min, respectively. **6FPI** with planar linkage group exhibited DRAM behavior while the corresponding isomer **6FPI'** behaved insulator characteristic due to the sustaining of charge transfer complex is difficult. Furthermore, sulfonyl-containing polymers generally have longer retention time than 6F series polymers with the same linkage due to the stronger acceptor effect.

Experimental

Materials. 4,4'-dihydroxytriphenylamine (**1**),^{14a} 4,4'-Diaminotriphenylamine (**2**),^{14b} *N,N*-bis(3,4-dicarboxyphenyl)aniline dianhydride (**3**),^{14c} 2,5-bis(4-fluorophenyl)-1,3,4-

oxadiazole (**OXDF**),^{14d} and 4,4'-(Hexafluoroisopropylidene)bis(benzoyl chloride) (**6FAC**)^{14c} were synthesized according to previous literature. The electroactive TPA-based aromatic polyamide **6FPA**^{15a} and polyimides **6FPI**^{15b} and **6FPI**^{14c} were also prepared according to previous research. Acetonitrile (CH₃CN) (ACROS), *N,N*-dimethylacetamide (DMAc) (TEDIA), *N*-methyl-2-pyrrolidinone (NMP) (TEDIA), *o*-dichlorobenzene (TEDIA) and *m*-cresol (Alfa Aesar) were used without further purification. 2,2-Bis(3,4-dicarboxyphenyl)hexafluoropropane dianhydride (6FDA) (Chriskev) was purified by vacuum sublimation. Tetrabutylammonium perchlorate (TBAP) (ACROS) was recrystallized twice by ethyl acetate under nitrogen atmosphere and then dried in vacuo prior to use. All other reagents were used as received from commercial sources.

Preparation of Polyether OXPE. To a three necked 50 mL glass reactor was charged with diol monomer **1** (0.14 g, 0.5 mmol), **OXDF** (0.13 g, 0.5 mmol), 1.5 mL NMP, 1 mL toluene, and an excess of potassium carbonate (0.15 g, 0.75 mmol). The reaction mixture was heated at 150 °C for 3 h to remove water during the formation of phenoxide anions, and then heated at 170 °C for 1 h, 180 °C for 3 h, and finally heated at 190 °C for 1 h. After the reaction, the obtained polymer solution was poured slowly into 300 mL of acidified methanol/water (v/v = 1/1). The precipitate was collected by filtration, washed thoroughly with hot water and methanol, and dried under vacuum at 100 °C. The inherent viscosity and weight-average molecular weight (M_w) of the obtained polyether **OXPE** was 0.29 dL/g (measured at a concentration of 0.5 g/dL in DMAc at 30 °C) and 62,000, respectively. The FT-IR spectrum of **OXPE** film exhibited characteristic C=N stretching absorption bands at around 1500-1600, and 1232 cm⁻¹ (C-O-C stretching).

Preparation of Polyester 6FPET. A mixture of 0.15 g (0.53 mmol) diol monomer **1** and 0.18 g (0.53 mmol) **6FAC** in 1.5 mL of *o*-dichlorobenzene was heated with stirring at 180 °C for 15 h under nitrogen. The solution thus obtained was poured into 300 mL of methanol. The yield of the polymer was 0.29 g (98%), and the inherent viscosity was 0.27 dL/g in DMAc. The weight-average molecular weight (M_w) of **6FPET** was 76,000. The IR spectrum (film) showed an absorption at 1737 cm⁻¹ (C = O).

Polymer Properties Measurements. Fourier transform infrared (FT-IR) spectra were recorded on a PerkinElmer Spectrum 100 Model FT-IR spectrometer. The inherent viscosities were determined at 0.5 g/dL concentration using Tamson TV-2000 viscometer at 30 °C. Gel permeation chromatographic (GPC) analysis was carried out on a Waters chromatography unit interfaced with a Waters 2410 refractive index detector. Two Waters 5 μm Styragel HR-2 and HR-4 columns (7.8 mm I. D. × 300 mm) were connected in series with NMP as the

eluent at a flow rate of 0.5 mL/min at 40 °C and were calibrated with polystyrene standards. Thermogravimetric analysis (TGA) was conducted with TA SDT Q600. Experiments were carried out on approximately 6–8 mg film samples heated in flowing nitrogen or air (flow rate = 20 cm³/min) at a heating rate of 20 °C/min. Differential scanning calorimetry (DSC) analyses were performed on a PerkinElmer Pyris 1 DSC at a scan rate of 10 °C/min in flowing nitrogen (20 cm³/min). Electrochemistry was performed with a CH Instruments 611B electrochemical analyzer. Voltammograms were presented with the positive potential pointing to the left and with increasing anodic currents pointing downwards. Cyclic voltammetry (CV) was conducted with a three-electrode cell in which ITO (polymer films area about 0.5 cm x 1.1 cm) was used as a working electrode. A platinum wire was used as an auxiliary electrode. All cell potentials were taken by using a homemade Ag/AgCl, KCl (sat.) reference electrode. UV-visible absorption was recorded on UV-visible spectrophotometer (Hitachi U-4100).

Fabrication and Measurement of the Memory Device. The memory device was fabricated with the configuration of ITO/polymer/Al as shown in Scheme 1. The ITO glass used for memory device was cleaned by ultrasonication with water, acetone, and isopropanol each for 15 min. DMAc solutions of TPA-based aromatic polymers (15-25 mg/mL) were first filtered through 0.45 μm pore size of PTFE membrane syringe filter. Then, 250 μL of the filtered solution was spin-coated onto the ITO glass at a rotation rate of 1000 rpm for 60 s and kept at 100 °C for 10 min under nitrogen. The thicknesses of thin films prepared by DMAc solutions with different polymer concentration were determined by alpha-step profilometer. A 300-nm-thick Al top electrode was thermally evaporated through the shadow mask (recorded device units of 0.5 × 0.5 mm² in size) at a pressure of 10⁻⁷ torr with a uniform depositing rate of 3-6 Å/s. The electrical characterization of the memory device was performed by a Keithley 4200-SCS semiconductor parameter analyzer equipped with a Keithley 4205-PG2 arbitrary waveform pulse generator. ITO was used as common electrode and Al was the electrode for applying voltage during the sweep.

Molecular Simulation. Molecular simulations in this study were carried out with the Gaussian 09 program package. Equilibrium ground state geometry and electronic properties of basic unit of TPA-based aromatic polymers were optimized by means of the density functional theory (DFT) method at the B3LYP level of theory (Becke's three-parameter density functional theory using the Lee-Yang-Parr correlation functional) with the 6-31G(d) basic set.

Acknowledgement

We gratefully acknowledge the financial support of this research through the National Science Council of Taiwan.

Electronic Supplementary Information (ESI) available: Figure: IR spectra, TGA thermograms, and DSC traces of polyether OXPE and polyester 6FPET. Reduction cyclic voltammetric diagrams of **6FPI** and **6FPI'**, and simulation results of TPA-based sulfonyl-containing polymers. Table: Molecular weights and solubility behavior.

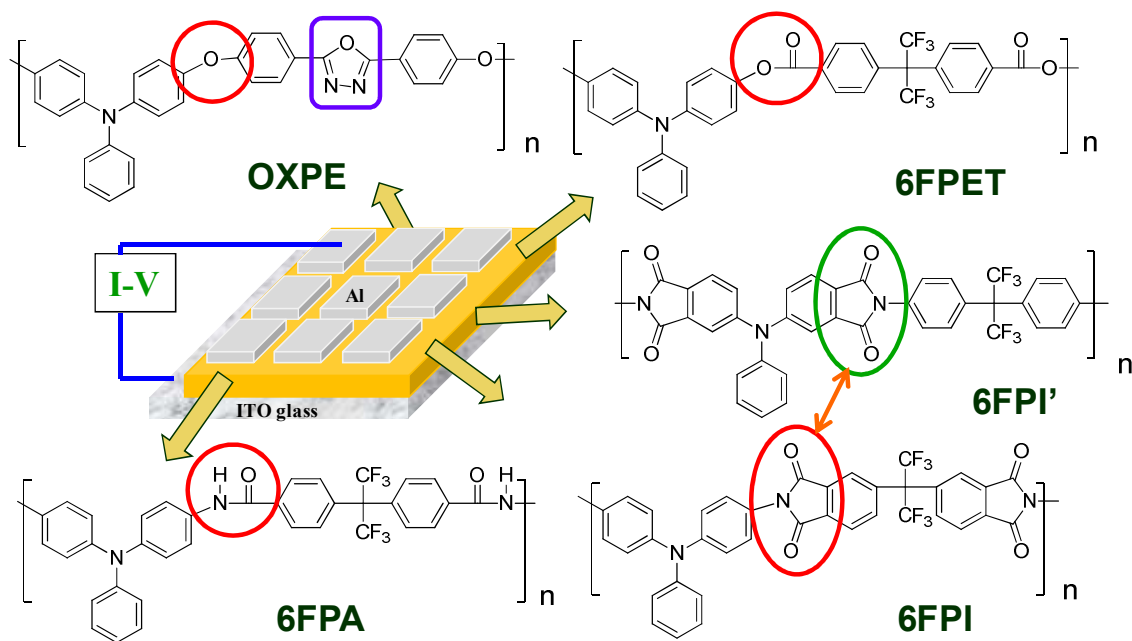
References and Notes

1. (a) P. O. Sliva, G. Dir and C. Griffiths, *J. Non-Cryst. Solids*, 1970, **2**, 316-333; (b) Q. D. Ling, D. J. Liaw, C. X. Zhu, D. S. H. Chan, E. T. Kang and K. G. Neoh, *Prog. Polym. Sci.*, 2008, **33**, 917-978; (c) S. Moller, C. Perlov, W. Jackson, C. Taussig and S. R. Forrest, *Nature*, 2003, **426**, 166-169; (d) J. C. Scott and L. D. Bozano, *Adv. Mater.*, 2007, **19**, 1452-1463.
2. (a) A. Stikeman, *Technol. Rev.*, 2002, 31-31; (b) P. Heremans, G. Gelinck, H. Muller, R. Baeg, K. J. Kim, D. Y. Noh and Y. Y. *Chem. Mater.*, 2011, **23**, 341-358.
3. (a) B. Cho, T. W. Kim, S. Song, Y. Ji, M. Jo, H. Hwang, G. Y. Jung and T. Lee, *Adv. Mater.*, 2010, **22**, 1228-1232; (b) T. W. Kim, D. F. Zeigler, O. Acton, H. L. Yip, H. Ma and A. K. Y. Jen, *Adv. Mater.*, 2012, **24**, 828-833; (c) R. J. Tseng, J. X. Huang, J. Ouyang, R. B. Kaner and Y. Yang, *Nano Lett.*, 2005, **5**, 1077-1080; (d) C. X. Wu, F. S. Li, T. L. Guo and T. W. Kim, *Org. Electron.*, 2012, **13**, 178-183.
4. (a) Q. D. Ling, F. C. Chang, Y. Song, C. X. Zhu, D. J. Liaw, D. S. H. Chan, E. T. Kang and K. G. Neoh, *J. Am. Chem. Soc.*, 2006, **128**, 8732-8733; (b) C. L. Liou and W. C. Chen, *Polym. Chem.*, 2011, **2**, 2169-2174.
5. (a) X. D. Zhuang, Y. Chen, G. Liu, P. P. Li, C. X. Zhu, E. T. Kang, K. G. Noeh, B. Zhang, J. H. Zhu and Y. X. Li, *Adv. Mater.*, 2010, **22**, 1731-1735; (b) X. D. Zhuang, Y. Chen, B. X. Li, D. G. Ma, B. Zhang and Y. Li, *Chem. Mater.*, 2010, **22**, 4455-4461; (c) Y. G. Ko, W. Kwon, D. M. Kim, K. Kim, Y. S. Gal and M. Ree, *Polym. Chem.*, 2012, **3**, 2028-2033; (d) W. Lin, H. Sun, S. Liu, H. Yang, S. Ye, W. Xu, Q. Zhao, X. Liu and W. Huang, *Macromol. Chem. Phys.*, 2012, **213**, 2472-2478; (e) S. J. Liu, W. P. Lin, M. D. Yi, W. J. Xu, C. Tang, Q. Zhao, S. H. Ye, X. M. Liu and W. Huang, *J. Mater. Chem.*, 2012, **22**,

- 22964-22970; (f) S. Baek, D. Lee, J. Kim, S. H. Hong, O. Kim and M. Ree, *Adv. Funct. Mater.*, 2007, **17**, 2637-2644; (g) H. C. Wu, A. D. Yu, W. Y. Lee, C. L. Liu and W. C. Chen, *Chem. Commun.*, 2012, **48**, 9135-9137.
6. (a) B. Zhang, G. Liu, Y. Chen, C. Wang, K. G. Neoh, T. Bai and E. T. Kang, *ChemPlusChem*, 2012, **77**, 74-81; (b) S. J. Liu, P. Wang, Q. Zhao, H. Y. Yang, J. Wong, H. B. Sun, X. C. Dong, W. P. Lin and W. Huang, *Adv. Mater.* 2012, **24**, 2901-2905; (c) S. G. Hahm, N. G. Kang, W. Kwon, K. Kim, Y. K. Ko, S. Ahn, B. G. Kang, T. Chang, J. S. Lee and M. Ree, *Adv. Mater.* 2012, **24**, 1062-1066; (d) Y. K. Fang, C. L. Liu, G. Y. Yang, P. C. Chen and W. C. Chen, *Macromolecules*, 2011, **44**, 2604-2612; (e) S. J. Liu, P. Wang, Q. Zhao, H. Y. Yang, J. Wong, H. B. Sun, X. C. Dong, W. P. Lin and W. Huang, *Adv. Mater.*, 2012, **24**, 2901-2905.
7. (a) A. D. Yu, C. L. Liu and W. C. Chen, *Chem. Commun.*, 2012, **48**, 383-385; (b) D. B. Velusamy, S. K. Hwang, R. H. Kim, G. Song, S. H. Cho, I. Bae and C. Park, *J. Mater. Chem.*, 2012, **22**, 25183-25189; (c) B. Zhang, Y. Chen, G. Liu, L. Q. Xu, J. Chen, C. X. Zhu, K.G. Neoh and E. T. Kang, *J. Polym. Sci. Part A: Polm. Chem.*, 2012, **50**, 378-387; (d) M. A. Khan, U. S. Bhansali, D. Cha and H. N. Alshareef, *Adv. Funct. Mater.*, 2012, DOI: 10.1002/adfm.201202724; (e) J. C. Chen, C. L. Liu, Y. S. Sun, S.H. Tungd and W. C. Chen, *Soft Matter.*, 2012, **8**, 526-535; (f) S. Gao, C. Song, C. Chen, F. Zeng and F. Pan, *J. Phys. Chem. C*, 2012, **116**, 17955-17959; (g) C. J. Chen, Y. C. Hu and G. S. Liou, *Chem. Commun.*, 2013, **49**, 2804-2806; (h) L. Q. Xu, B. Zhang, K. G. Neoh, E. T. Kang and G. D. Fu, *Macromol. Rapid Commun.*, 2013, **34**, 234-238; (i) M. A. Mamo, A. O. Sustaita, N. J. Coville, and I. A. Hummelgen, *Org. Electron.*, 2013, **14**, 175-181.
8. (a) T. Kurosawa, Y. C. Lai, T. Higashihara, M. Ueda, C. L. Liu and W. C. Chen, *Macromolecules*, 2012, **45**, 4556-4563; (b) Y. Q. Li, R. C. Fang, A. M. Zheng, Y. Y. Chu, X. Tao, H. H. Xu, S. J. Ding and Y. Z. Shen, *J. Mater. Chem.*, 2011, **21**, 15643-15654; (c) T. J. Lee, Y. G. Ko, H. J. Yen, K. Kim, D. M. Kim, W. Kwon, S. G. Hahm, G. S. Liou and M. Ree, *Polym. Chem.*, 2012, **3**, 1276-1283; (d) F. Chen, G. Tian, L. Shi, S. Qi and D. Wu, *RSC Advances*, 2012, **2**, 12879-12885; (e) Y. Liu, Y. Zhang, Q. Lan, S. Liu, Z. Qin, L. Chen, C. Zhao, Z. Chi, J. Xu and J. Economy, *Chem. Mater.*, 2012, **24**, 1212-1222; (f) T. Kurosawa, T. Higashihara and M. Ueda, *Polym. Chem.*, 2013, **4**, 16-30; (g) N. H. You, C. C. Chueh, C. L. Liu, M. Ueda and W. C. Chen, *Macromolecules*, 2009, **42**, 4456-4463; (h) S. G. Hahm, S. Choi, S. H. Hong, T. J. Lee, S. Park, D. M. Kim, W. S. Kwon, K. Kim, O. Kim and M. Ree, *Adv. Funct. Mater.*, 2008, **18**, 3276-3282; (i) Q. Liu, K. Jiang, Y. Wen, J. Wang, J. Luo and Y. Song, *Appl. Phys. Lett.*, 2010, **97**, 253304-1-

- 253304-3; (j) Y. Li, Y. Chu, R. Fang, S. Ding, Y. Wang, Y. Shen and A. Zheng, *Polymer*, 2012, **53**, 229-240.
9. (a) C. J. Chen, H. J. Yen, W. C. Chen and G. S. Liou, *J. Mater. Chem.*, 2012, **22**, 14085-14093; (b) T. J. Lee, C. W. Chang, S. G. Hahm, K. Kim, S. Park, D. M. Kim, J. Kim, W. S. Kwon, G. S. Liou and M. Ree, *Nanotechnology*, 2009, **20**, 135204-1-135204-7; (c) D. M. Kim, S. Park, T. J. Lee, S. G. Hahm, K. Kim, J. C. Kim, W. Kwon and M. Ree, *Langmuir*, 2009, **25**, 11713-11719; (d) Y. C. Hu, C. J. Chen, H. J. Yen, K. Y. Lin, J. M. Yeh, W. C. Chen and G. S. Liou, *J. Mater. Chem.*, 2012, **22**, 20394-20402; (e) K. Kim, H. J. Yen, Y. G. Ko, C. W. Chang, W. Kwon, G. S. Liou and M. Ree, *Polymer*, 2012, **53**, 4135-4144; (f) Y. G. Ko, W. Kwon, H. J. Yen, C. W. Chang, D. M. Kim, K. Kim, S. G. Hahm, T. J. Lee, G. S. Liou and M. Ree, *Macromolecules*, 2012, **45**, 3749-3758; (g) T. J. Lee, Y. G. Ko, H. J. Yen, K. Kim, D. M. Kim, W. Kwon, S. G. Hahm, G. S. Liou and M. Ree, *Polym. Chem.*, 2012, **3**, 1276-1283; (h) K. Kim, S. Park, S. G. Hahm, T. J. Lee, D. M. Kim, J. C. Kim, W. Kwon, Y. G. Ko and M. Ree, *J. Phys. Chem. B*, 2009, **113**, 9143-9150; (i) K. L. Wang, Y. L. Liu, J. W. Lee, K. G. Neoh and E. T. Kang, *Macromolecules*, 2010, **43**, 7159-7164; (j) Y. Li, R. Fang, S. Ding and Y. Shen, *Macromol. Chem. Phys.*, 2011, **212**, 2360-2370; (k) K. L. Wang, Y. L. Liu, I. H. Shih, K. G. Neoh and E. T. Kang, *J. Polym. Sci. Part A: Polym. Chem.*, 2010, **48**, 5790-5800; (l) A. D. Yu, T. Kurosawa, Y. C. Lai, T. Higashihara, M. Ueda, C. L. Liu and W. C. Chen, *J. Mater. Chem.*, 2012, **22**, 20754-20763; (m) D. M. Kim, Y. G. Ko, J. K. Choi, K. Kim, W. Kwon, J. Jung, T. H. Yoon and M. Ree, *Polymer*, 2012, **53**, 1703-1710.
10. (a) C. W. Chang, G. S. Liou and S. H. Hsiao, *J. Mater. Chem.*, 2007, **17**, 1007-1015; (b) H. J. Yen and G. S. Liou, *Chem. Mater.*, 2009, **21**, 4062-4070; (c) H. J. Yen, H. Y. Lin and G. S. Liou, *Chem. Mater.*, 2011, **23**, 1874-1882; (d) G. S. Liou, C. W. Chang, H. M. Huang and S. H. Hsiao, *J. Polym. Sci. Part A: Polym. Chem.*, 2007, **45**, 2004-2014.
11. (a) C. J. Chen, H. J. Yen, W. C. Chen and G. S. Liou, *J. Polym. Sci. Part A: Polym. Chem.*, 2011, **49**, 3709-3718; (b) C. J. Chen, Y. C. Hu and G. S. Liou, *Chem. Commun.* 2013, **49**, 2536-2538.
12. (a) Y. L. Liu, K. L. Wang, G. S. Huang, C. X. Zhu, E. S. Tok, K. G. Neoh and E. T. Kang, *Chem. Mater.*, 2009, **21**, 3391-3399; (b) T. Kuorosawa, C. C. Chueh, C. L. Liu, T. Higashihara, M. Ueda and W. C. Chen, *Macromolecules*, 2010, **43**, 1236-1244; (c) B. L. Hu, F. Zhuge, X. J. Zhu, S. S. Peng, X. X. Chen, L. Pan, Q. Yan and R. W. Li, *J. Mater. Chem.*, 2012, **22**, 520-526.

13. (a) G. S. Liou, H. J. Yen and M. C. Chiang, *J. Polym. Sci. Part A: Polym. Chem.*, 2009, **47**, 5378-5385; (b) H. J. Yen and G. S. Liou, *Org. Electron.*, 2010, **11**, 299-310.
14. (a) M. Faccini, M. Balakrishnan, M. B. J. Diemeer, R. Torosantucci, A. Driessen, D. W. Reinhoudt and W. Verboom, *J. Mater. Chem.*, 2008, **18**, 5293-5300; (b) Y. Oishi, H. Takado, M. Kakimoto and Y. Imai, *J. Polym. Sci. Polym. Chem. Ed.*, 1990, **28**, 1763-1769; (c) W. Li, S. Li, Q. Zhang and S. Zhang, *Macromolecules*, 2007, **40**, 8205-8211; (d) J. L. Hedrick and R. Twieg, *Macromolecules*, 1992, **25**, 2021-2025; (e) C. S. Wu, S. L. Lee and Y. Chen, *J. Polym. Sci. Part A: Polym. Chem.*, 2011, **49**, 3099-3108.
15. (a) S. H. Cheng, S. H. Hsiao, T. H. Su and G. S. Liou, *Macromolecules*, 2005, **38**, 307-316; (b) H. Su, S. H. Hsiao and G. S. Liou, *J. Polym. Sci. Part A: Polym. Chem.*, 2005, **43**, 2085-2098.
16. Q. D. Ling, Y. Song, S. L. Lim, E. Y. H. Teo, Y. P. Tan and C. X. Zhu, *Angew. Chem. Int. Ed.*, 2006, **45**, 2947-2951.



Scheme 1. Chemical structures of TPA-based aromatic polymers and schematic diagram of the memory device consisting of a polymer thin film sandwiched between an ITO bottom electrode and an Al top electrode.

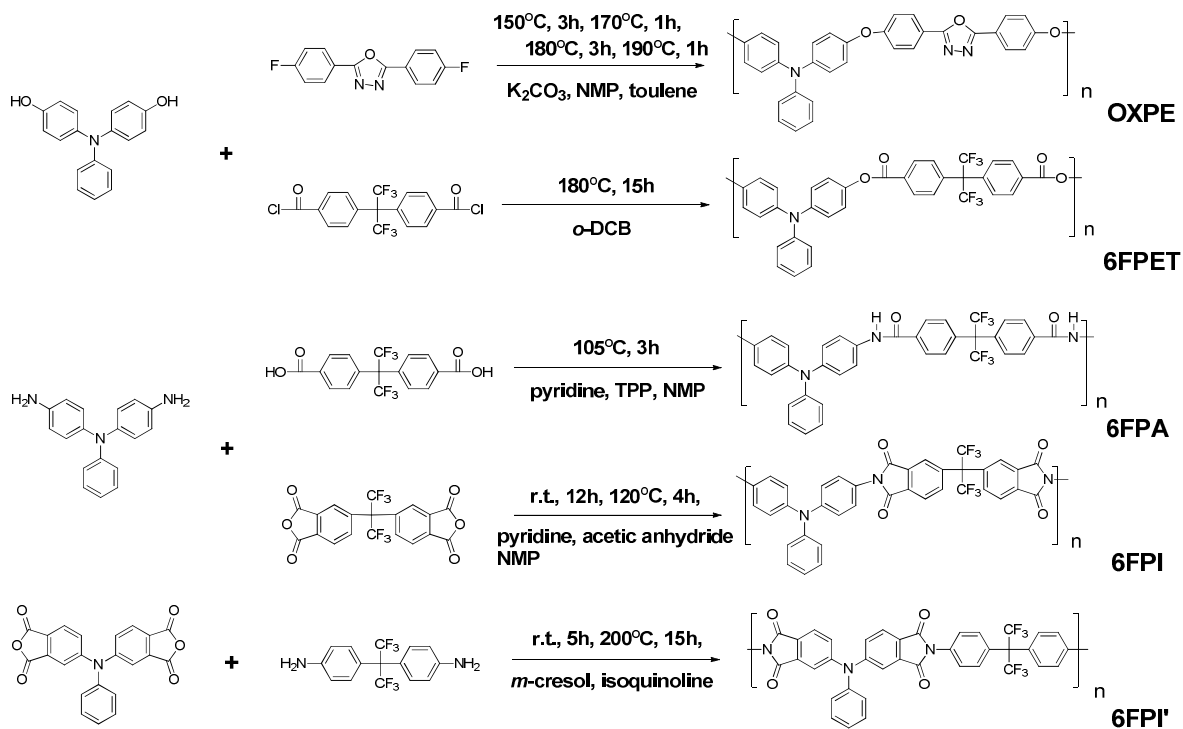


Figure 1. Synthesis methods of OXPE, 6FPET, 6FPA, 6FPI, and 6FPI'.

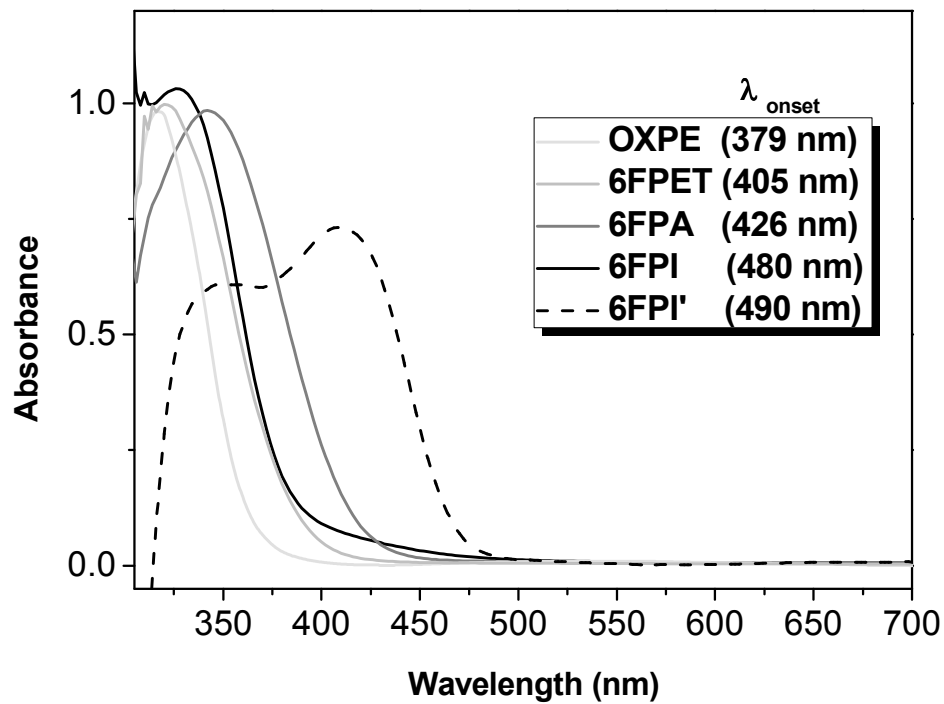


Figure 2. UV-visible absorption spectra of OXPE, 6FPET, 6FPA, 6FPI, and 6FPI'.

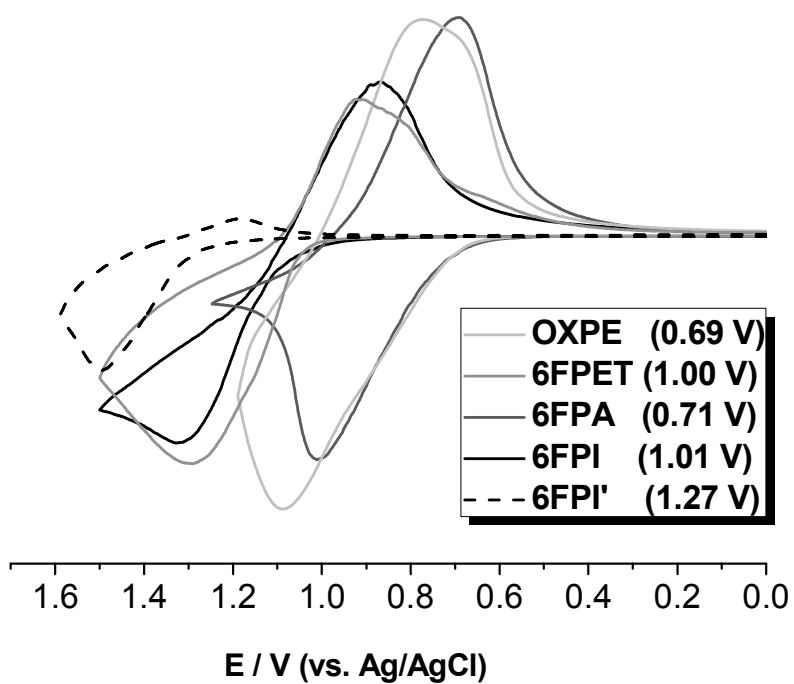


Figure 3. Cyclic voltammetric diagrams of **OXPE**, **6FPET**, **6FPA**, **6FPI**, and **6FPI'** films on an ITO-coated glass substrate over cyclic scans.

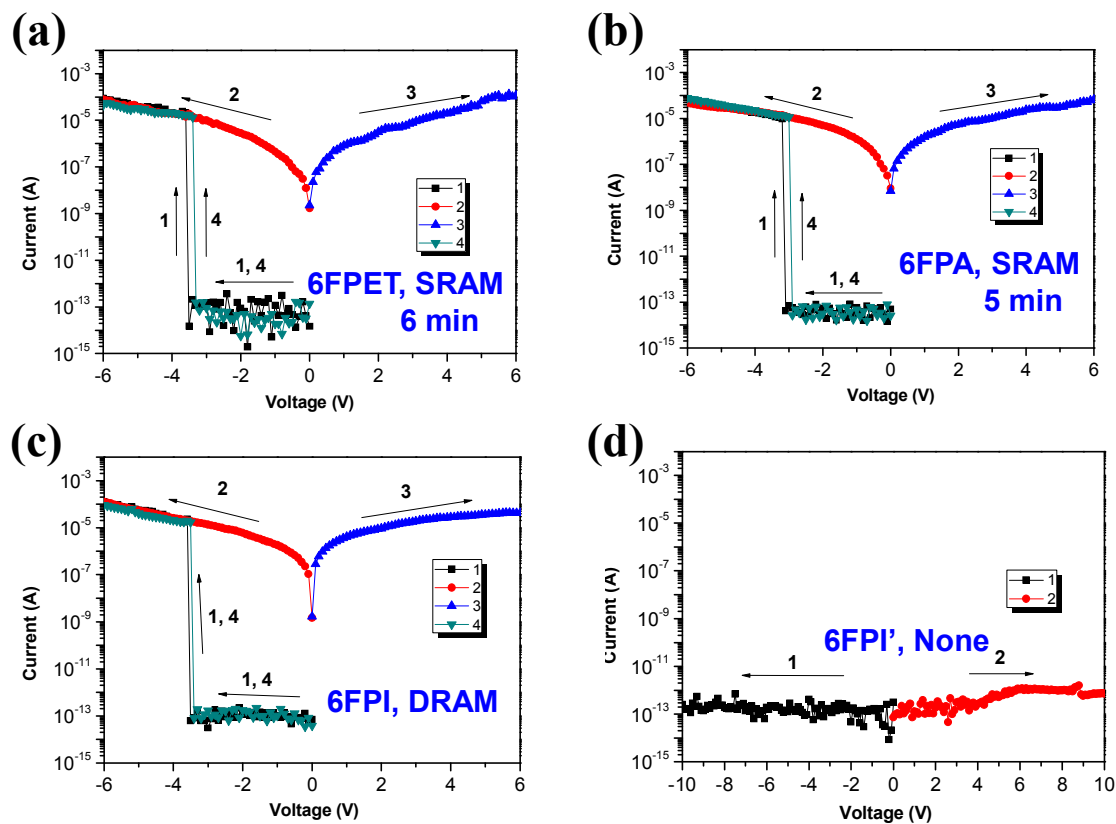


Figure 4. Current-voltage (I-V) characteristics of the ITO/Polymer (50 ± 3 nm)/Al memory device. (a) 6FPET (b) 6FPA (c) 6FPI (d) 6FPI'.

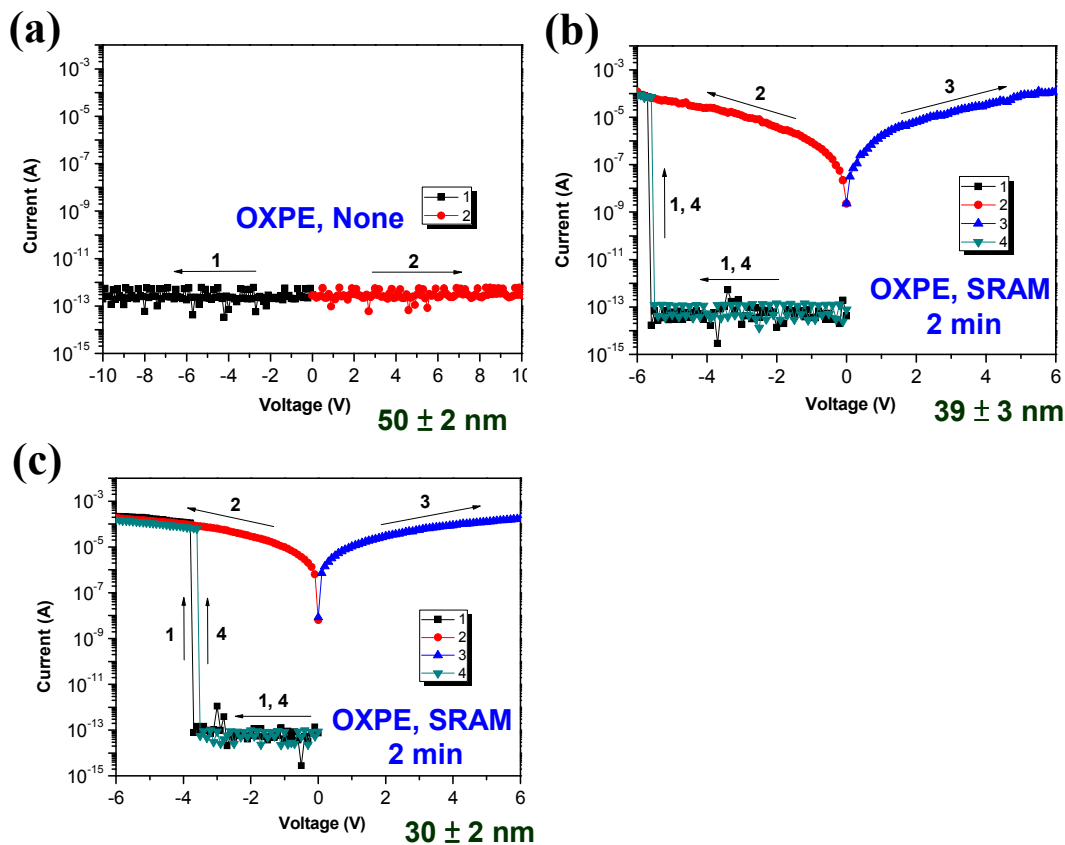


Figure 5. Current-voltage (I-V) characteristics of the ITO/OXPE/Al memory device with different OXPE film thickness around (a) 50 nm (b) 40 nm (c) 30 nm.

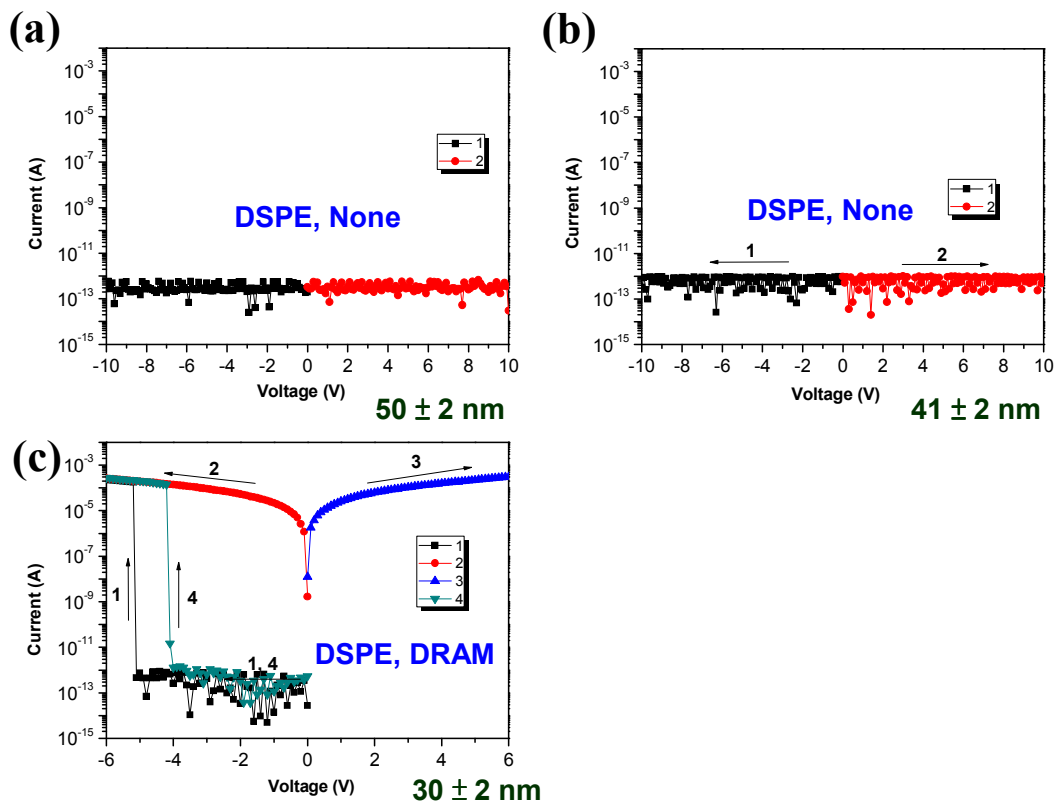


Figure 6. Current-voltage (I-V) characteristics of the ITO/DSPE/Al memory device with different OXPE film thickness around (a) 50 nm (b) 40 nm (c) 30 nm.

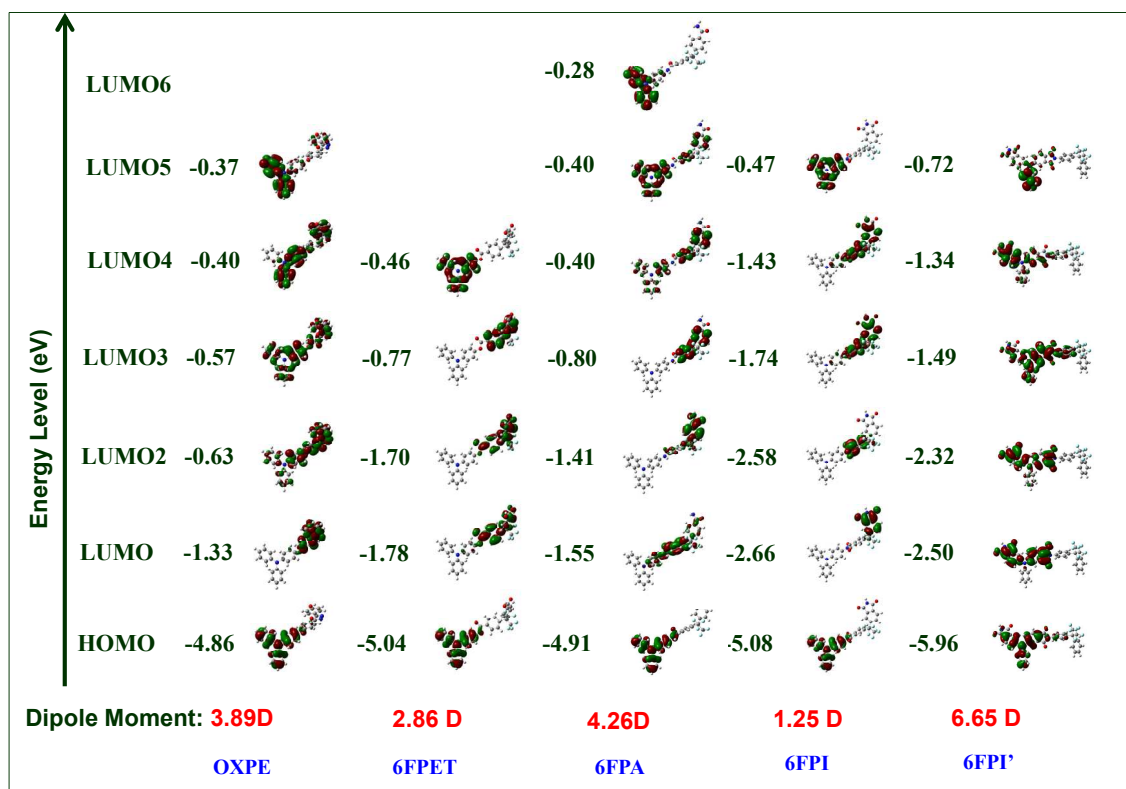


Figure 7. Calculated molecular orbitals and corresponding energy levels of the basic units (BU) for **OXPE**, **6FPET**, **6FPA**, **6FPI**, and **6FPI'**.

		Flexible Linkage				Planar Linkage	
Acceptor Effect		OXPE (30 nm)	OXPE (40 nm)	OXPE	DSPET	DSPA	DSPI
		SRAM 2 min	SRAM 2 min	None	SRAM 11 min	SRAM 8 min	SRAM 4 min
		DSPE (30 nm)	DSPE (40 nm)	DSPE	6FPET	6FPA	6FPI
		DRAM	None	None	SRAM 6 min	SRAM 5 min	DRAM
						6FPI'	None

Figure 8. Memory properties of TPA-based aromatic polymers. A standard thickness (50 nm) of polymer film was used without specific mention.

Table 1. Thermal Properties

Polymer ^a	T_g^b (°C)	T_d^5 (°C) ^c		T_d^{10} (°C) ^c		R_{w800} (%) ^d	LOI ^e
		N ₂	Air	N ₂	Air		
OXPE	206	460	460	500	500	49	37
6FPET	193	450	420	480	465	50	38

^a The polymer film samples were heated at 300 °C for 1 h prior to all the thermal analyses.

^b Midpoint temperature of baseline shift on the second DSC heating trace (rate: 20 °C /min) of the sample after quenching from 400 °C to 50 °C (rate: 200 °C /min) in nitrogen

^c Temperature at which 5 % and 10% weight loss occurred, respectively, recorded by TGA at a heating rate of 20 °C/min and a gas flow rate of 20 cm³/min.

^d Residual weight percentages at 800 °C under nitrogen flow.

^e LOI: Limiting Oxygen Index = (17.5 + 0.4×char yield).

Table 2. Redox Potentials and Energy Levels of Polymers

Polymer	Thin film (nm)	Oxidation potential (V) ^a	E_g (eV) ^b	HOMO (eV) ^c	LUMO ^{opt} (eV) ^d
	λ_{onset}	E_{onset}			
OXPE	379	0.69	3.27	5.13	1.86
6FPET	405	1.00	3.06	5.44	2.38
6FPA	426	0.71	2.91	5.15	2.24
6FPI	480	1.01	2.58	5.45	2.87 (3.50) ^e
6FPI'	490	1.27	2.53	5.71	3.18 (3.46) ^e
DSPE	361	0.68	3.43	5.12	1.69
DSPET	458	1.01	2.71	5.45	2.74
DSPA	496	0.74	2.50	5.18	2.68
DSPI	567	1.02	2.19	5.46	3.27

^a From cyclic voltammograms versus Ag/AgCl in CH₃CN.

^b The data were calculated from polymer films by the equation: $E_g = 1240/\lambda_{onset}$ (energy gap between HOMO and LUMO).

^c The HOMO energy levels were calculated from cyclic voltammetry and were referenced to ferrocene (4.8 eV; $E_{onset} = 0.36$ V).

^d LUMO^{opt} (LUMO energy levels calculated from optical method): Difference between HOMO^{EC} and E_g^{opt} .

^e The LUMO energy levels were calculated from cyclic voltammetry and were referenced to ferrocene (4.8 eV ; $E_{1/2} = 0.52$ V in DMF).

For Table of Contents use only

Linkage and Acceptor Effect on Diverse Memory Behavior of Triphenylamine-Based Aromatic Polymers

Chih-Jung Chen, Yi-Cheng Hu, and Guey-Sheng Liou*

New functional triphenylamine-based aromatic polyether **OXPE**, new polyester **6FPET**, polyamide **6FPA**, polyimide **6FPI**, and corresponding isomer **6FPI'** with different linkage groups were synthesized and used for memory device application. Besides, sulfonyl-containing polymers were also added into discussion.

